J Mater Sci (2007) 42:2143–2149
DOI 10.1007/s10853-006-1298-7

Thermoelectric properties of Zn_4Sb_3 processed by sintering of cold pressed compacts and hot pressing

Soon-Chul Ur · Il-Ho Kim · Philip Nash

Received: 7 April 2005 / Accepted: 20 January 2006 / Published online: 15 December 2006

Abstract Sintering of cold die-pressed compacts and hot pressing have been used in order to produce high efficiency, thermoelectric ε-Zn_4Sb_3 bulk specimens. Single-phase Zn_4Sb_3 was successfully produced by sintering of cold die-pressed compacts using mixed elemental powders, and subsequent hot pressing produced single-phase, bulk specimens without microcracks. Phase transformations in this alloy system during synthesis were investigated using DSC, XRD and SEM. Thermoelectric properties as a function of temperature were investigated from room temperature to 600 K and compared with results of other studies. Transport properties at room temperature were evaluated. Thermoelectric properties of single phase Zn_4Sb_3 materials produced by the sintering of cold die-pressed compacts and hot pressing are comparable to the published data for alternate processing routes. Synthesis by sintering of cold die-pressed compacts and hot pressing offers a potential processing route to produce bulk Zn_4Sb_3.

Introduction

A great deal of attention has been diverted toward Zn_4Sb_3 thermoelectric materials owing to their attractive properties such as a high figure of merit value in an intermediate temperature range (450–650 K) and relatively low cost [1–3]. They can potentially substitute for high performance lead tellurides, which contain environmentally harmful lead [2, 3]. Hexagonal rhombohedric Zn_4Sb_3 compound shows an intrinsic p-type semiconducting behavior [4] with high value of the figure of merit, ZT = 1.3 at 673 K [2]. The figure of merit is defined as $ZT = \alpha^2\sigma T/\lambda$, where α is the Seebeck coefficient, σ is the electrical conductivity, λ is the thermal conductivity and T is the temperature in Kelvin.

Several processing methods have been used to produce Zn_4Sb_3. They include melting in controlled atmosphere followed by granulation and hot consolidation [1–3], mechanical alloying for powder synthesis [5], and bulk mechanical alloying followed by hot pressing [6]. However, the preparation of polycrystalline ε-Zn_4Sb_3 involves rather complicated processes and frequently results in the formation of undesirable metallic phases such as orthorhombic β-ZnSb and orthorhombic δ-Zn_4Sb_3 [1, 3, 5]. In high temperature preparation processes such as ingot casting or single crystal growth of Zn_4Sb_3, it is very common that a large number of cracks are found due to the volumetric changes and mismatch in thermal expansion coefficient during the phase transition between ε and δ at 765 K [1]. Compositional changes are also frequently observed during processing since Zn_4Sb_3 decomposes into ZnSb and Zn at high temperature due to the relatively poor stability of the compound [7, 8]. In

S.-C. Ur (✉) · I.-H. Kim
Department of Materials Science & Engineering/Research Center for Sustainable ECo-Devices & Materials,
Chungju National University, Chungju,
Chungbuk 380-702, S. Korea
e-mail: scur@chungju.ac.kr

P. Nash
Thermal Processing Technology Center,
Illinois Institute of Technology,
Chicago, IL 60616, USA

order to address these problems, an approach is suggested, which involves solid state synthesis with prolonged thermal annealing at a temperature somewhat below the polymorphic transition temperature, at 673–723 K [1]. It is well established that intermetallic phases can be prepared by means of various solid state syntheses including mechanical alloying (MA) [9], direct synthesis [10] and repeated cold rolling and annealing [11].

In order to produce crack free, bulk specimens having good homogeneity, solid state synthesis consisting of cold compaction of elemental powders, sintering and hot pressing has been used in this work. However, when the starting materials are exposed to high temperature processing, some compositional changes are expected due to the evaporation of Zn [6]. Thus, as starting materials, stoichiometric compositions as well as Zn rich compositions, to compensate for Zn evaporation, were used. Thermoelectric properties as a function of temperature from room temperature to 600 K were measured and compared with the results of previously published studies. Some physical and electronic transport properties at room temperature were also evaluated and discussed.

Experimental procedure

Appropriate elemental powder mixtures of –325 mesh Sb (99.9%) and –325 mesh Zn (99.9%) were prepared for stoichiometric ε-Zn_4Sb_3 and nominally 3.5–7.0 at.% Zn rich mixtures as presented in Table 1. Powder mixtures were cold pressed in a stainless steel die with an internal diameter of 25.4 mm with a stress of 70 MPa. The cold die-pressed compacts were sintered in a tube furnace at 673 K under an Ar atmosphere for 24 h. The sintered part was crushed into powder, sieved to –270 mesh and hot pressed in a cylindrical high strength graphite die with an internal diameter of 31.75 mm at 673 K using a stress of 70 MPa for 2–24 h under an Ar atmosphere.

Table 1 Sample designations and nominal compositions used in sintering of cold die-pressed compacts and hot pressing

Sample	Zn (at.%)	Sb (at.%)	Excess Zn (at.%) over stoichiometry
SC0	57.1429	42.8571	0
SC3	58.6429	41.3571	3.5
SC7	60.1429	39.8571	7.0

Note: SC stands for the sintering of cold compact and numbers after that are excess Zn percentage.

Differential scanning calorimetry (DSC), at a heating rate of 10 K/min, was used to investigate phase transformations in the alloys. X-ray diffraction (XRD) analyses were carried out on the powders as well as hot pressed specimen to determine the degree of alloying during each processing step. Scanning electron microscopy (SEM) and energy dispersive spectroscopy (EDS) were employed for microstructural characterization.

Thermoelectric properties as a function of temperature up to 600 K were evaluated for specimens synthesized by sintering of cold die-pressed compacts and hot pressing. Electrical conductivity (σ) was measured by the 4-point probe method. Seebeck coefficient (α) was determined by the constant temperature gradient method in which one end of the specimen was kept at a constant low temperature by a heat sink and the other end was heated by a small heater. The thermal emf (electromotive force) developed was measured with respect to the temperature gradient. Copper-constantan thermocouples were used to measure the temperatures of the hot and cold ends, and the thermal emf of the specimen with respect to copper was recorded. Thermoelectric power factor ($\theta = \alpha^2\sigma$) was obtained from the Seebeck coefficient and electrical conductivity. Electronic transport parameters at room temperature were evaluated; Hall coefficient (R_H), carrier concentration (p) and mobility (μ) were measured by the Van der Pauw method (1.64 T, 100 mA) [12].

Results and discussion

DSC for cold die-pressed compacts of premixed stoichiometric Zn_4Sb_3 was carried out up to 900 K as shown in Fig. 1. In the first DSC run, two exothermic peaks were observed at 411 K and 502 K. Similar exothermic peaks below 600 K were observed in mechanically alloyed powders [5]. It was claimed that an exothermic peak at 423 K related to the release of the energy of cold work in mechanically alloyed powders, and a peak at 533 K resulted from the phase transformation from the initially formed ZnSb phase to Zn_4Sb_3 phase [5]. However, relative DSC peak intensities in our study are stronger than those in the work by Izard et al [5] and shifted to lower temperatures. In order to investigate phase transformations regarding these exothermic peaks, cold die-pressed compacts of stoichiometric composition were sintered slightly above each of the two peak temperatures for 1 h, and the resultant phases were examined by XRD.

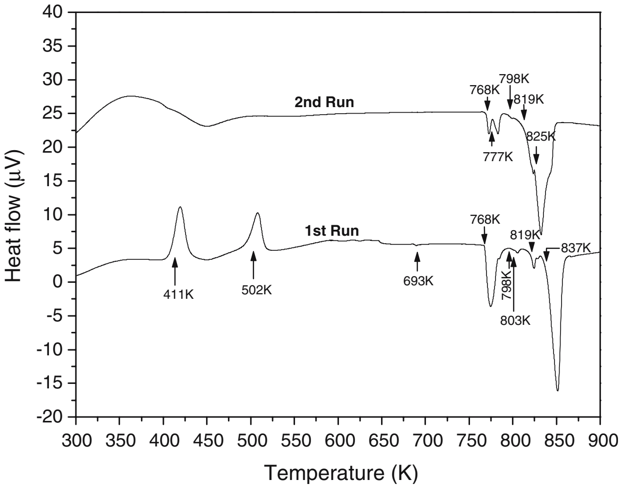

Fig. 1 DSC result of the cold die-pressed compact of stoichiometric composition of Zn_4Sb_3

Zn, Sb and Zn_4Sb_3 phases were identified in Fig. 2b and Zn, Sb, ZnSb and Zn_4Sb_3 phases were observed in Fig. 2c, indicating that the first peak in Fig. 1 represented the alloy formation of Zn_4Sb_3 and the second peak was for the ZnSb formation. This may be contrasted with the results from MA powders [5]. It is likely that the Zn content of samples in our work was lowered due to continuous evaporation during sintering since Zn with a higher vapor pressure will evaporate faster than Sb resulting in the formation of ZnSb rather than Zn_4Sb_3 above 502 K. Other endothermic peaks in Fig. 1 were shown to be consistent with the phase diagram published by Izard et al [5]. The peak at 693 K corresponds to the melting of remnant Zn, that at 768 K to the peritectoid reaction from ε phase to δ-Zn_4Sb_3 + ζ-Zn_3Sb_2 phases, the peak at 803 K corresponds to the transition from δ to δ', and the peak at 837 K to melting of the compound. However, a compositional shift from stoichiometry to an Sb-rich composition was found. For example, the peak 798 K corresponds to the transition from $\beta + \delta$ to $\beta + \delta'$ and at 819 K to the transition from $\beta + \delta'$ to $L + \delta'$. This result confirms that Zn evaporation takes place during DSC. In the second run of DSC using the same specimen, two exothermic peaks were no longer observed, suggesting that alloy formation was completed during one cycle of the DSC run.

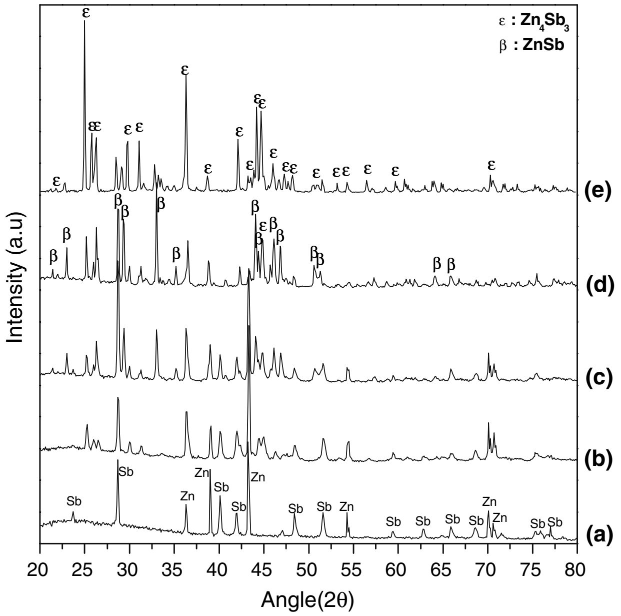

Fig. 2 XRD patterns of cold die-pressed samples of stoichiometric Zn_4Sb_3; (**a**) as-mixed, (**b**) sintered at 423 K/ 1 h, (**c**) sintered at 550 K/ 1 h, (**d**) sintered at 673 K/ 4 h, (**e**) sintered at 673 K/ 24 h

In order to investigate phase transformations on a larger scale for the cold die-pressed stoichiometric samples, sintering was carried out at 673 K for 4 and 24 h, and the resultant phases were examined by XRD as shown in Fig. 2d, e. From Fig. 2c, d, progressive development of Zn_4Sb_3 is shown after sintering at 673 K for 4 h but most of the phase formed is ZnSb. After 24 h of sintering at 673 K, most of the phase formed is Zn_4Sb_3, but some portion of ZnSb phase exists possibly due to Zn evaporation, as shown in Fig. 2e. It can be considered that Zn_4Sb_3 might be developed by either direct reaction of each element or by the reaction from ZnSb + Zn to Zn_4Sb_3 during sintering.

Since Zn evaporation is inevitable in the high temperature processing of this material, an appropriate amount of Zn addition to the stoichiometric composition was considered. In an attempt to produce single-phase bulk Zn_4Sb_3, powder mixture containing 3.5 at.% of excess Zn was cold compacted and sintered at 673 K for 2–24 h. Sintered samples show a volumetric expansion with a tendency of losing mechanical strength as in Fig. 3, due to volumetric changes accompanied by phase transition. The sintered compact has little bonding strength and tends to easily fall apart into powder.

Powders produced after sintering were mostly –270 mesh as shown in Fig. 4. XRD analysis revealed that powders consist of the single-phase Zn_4Sb_3, as shown in Fig. 5a. It is believed that the excess amount of Zn (3.5 at. %) added compensated for the Zn evaporation during sintering. Cold compaction of 7.0 at.% Zn excess powder mixtures was also attempted at the same condition, and resulted in Zn_4Sb_3 with a small amount of remnant Zn as shown in Fig. 6a.

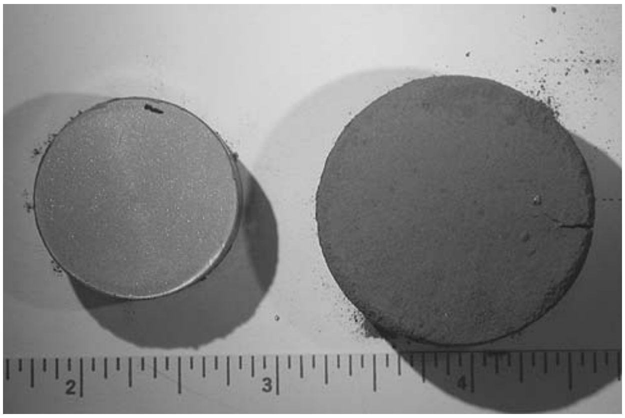

Fig. 3 Photographs of cold die-pressed compacts using nominally 3.5 at.% Zn rich powder mixtures; before sintering (left) and after sintering (right) at 673 K/24 h

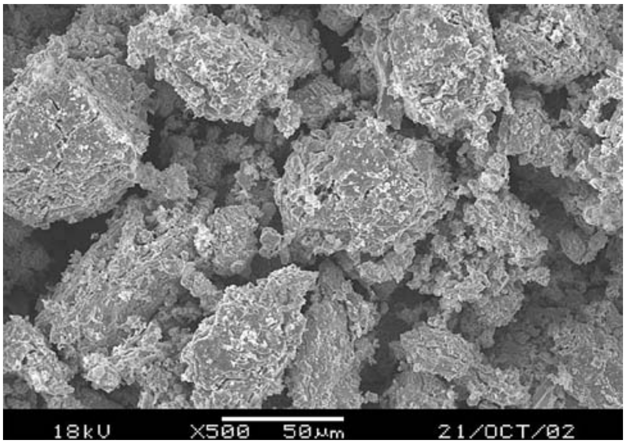

Fig. 4 SEM micrograph of sintered powders processed from the cold compaction of 3.5 at. % Zn rich powder mixtures

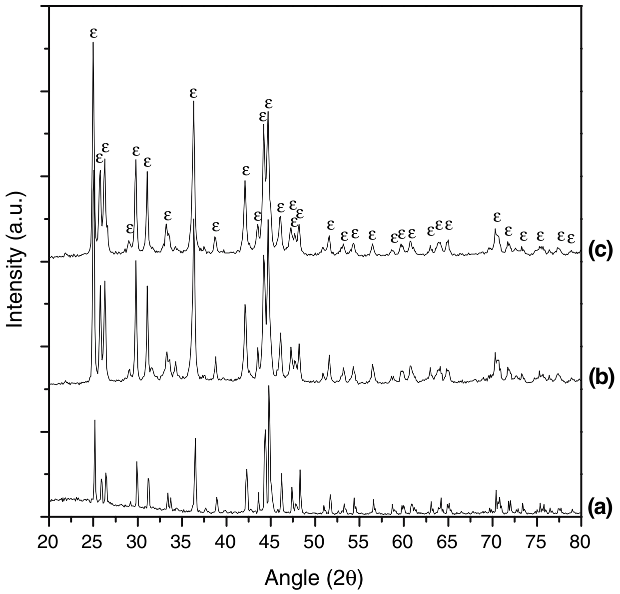

Fig. 5 XRD patterns of cold die-pressed compacts using normally 3.5 at. % Zn rich powder mixture; (**a**) crushed powders after sintering at 673 K/24 h, (**b**) hot pressed at 673 K/2 h using sintered powders, (**c**) hot pressed at 673 K/24 h using sintered powders

Sintered powders were then hot pressed at 673 K for 2–24 h. Relative densities and other related properties are presented in Table 2. In general, a relatively lower density was obtained by shorter time of hot pressing. Samples with a theoretical density of 94.7% consisting of a single phase were obtained using nominally 3.5 at.% Zn rich composition after 24 h of hot pressing, as presented in Fig. 7. XRD analysis revealed that specimens prepared by this process using nominally 3.5 at.% Zn rich composition were single-phase Zn_4Sb_3. EDS analysis also confirm single-phase Zn_4Sb_3 throughout the matrix. During hot pressing of the sintered powders using nominally 7 at.% Zn rich composition, peaks for excess Zn are not distinguishable in Fig. 6b, indicating continuous evaporation of excess Zn during the process. 93.3% of theoretical density samples consisting of mostly Zn_4Sb_3 were obtained using 7.0 at.% Zn rich composition by 2 h of hot pressing, but some remnant Zn was found.

Thermoelectric properties at room temperature are presented in Table 2, together with the properties of single-phase Zn_4Sb_3 produced by melting in a controlled atmosphere followed by hot pressing [2] which are provided for reference. Seebeck coefficients, $\alpha(\mu V/K)$, all show positive values, representing p-type

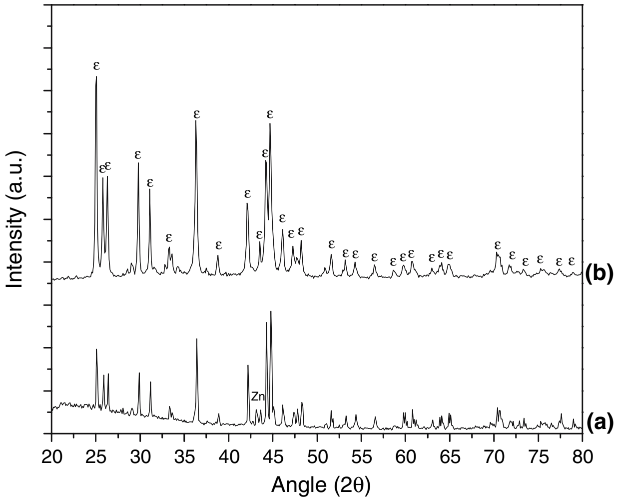

Fig. 6 XRD patterns of cold die-pressed compacts using normally 7.0 at. % Zn rich powder mixture; (**a**) crushed powders after sintering at 673 K/24 h, (**b**) hot pressed at 673 K/2 h using sintered powders

Table 2 Thermoelectric properties at room temperature for specimens produced by sintering of cold-pressed compacts and hot pressing

Sample	$\alpha(\mu V/K)$	$\sigma(\Omega^{-1}\ cm^{-1})$	$\theta(\mu W/cmK^2)$	Relative density(%)	Hv	phases	Remarks
Ref. [2]	113	500	6.4	96–98	–	ε	
SC0						ε	Powder
SC0HP2	50.2	139.6	0.35	93.6	145.0	$\varepsilon+\beta$	HP/2 h
SC3						ε	Powder
SC3HP2	85.4	498.8	3.6	86.1	135.3	ε	HP/2 h
SC3HP24	98.2	463.7	4.5	94.7	181.6	ε	HP/24 h
SC7						ε+Zn	Powder
SC7HP2	60.6	281.1	0.8	93.3	122	ε+Zn	HP/2 h

Note: HP stands for hot pressing, and numbers after HP represent are hot pressing time in hour.

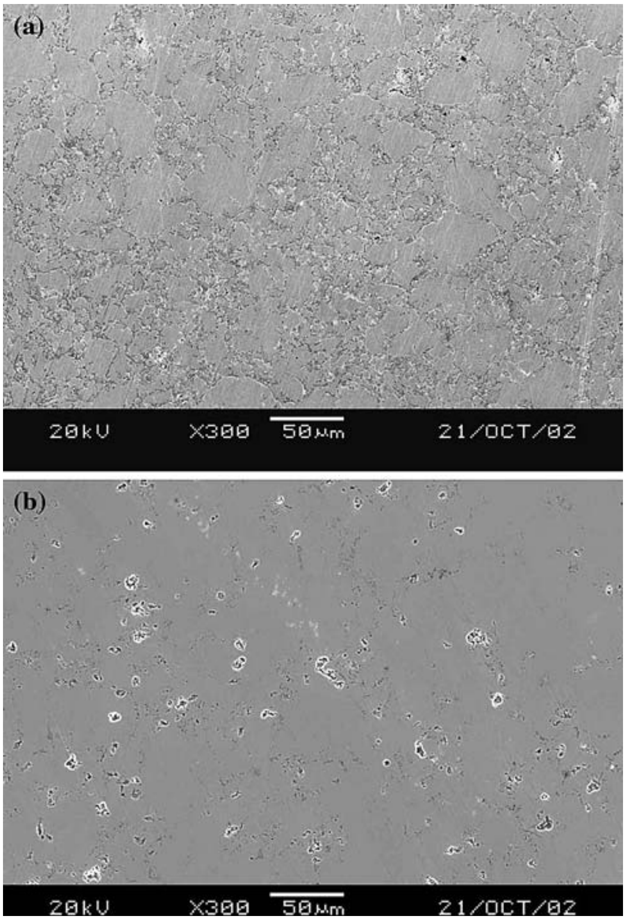

Fig. 7 SEM micrograph of hot pressed specimen using sintered powder with nominally 3.5 at.% Zn rich powders; (**a**) hot pressed at 673 K/2 h, (**b**) hot pressed at 673 K/24 h

conductivity. Seebeck coefficients and electrical conductivities of single-phase Zn_4Sb_3 are produced in this work comparable to the published data. In single-phase Zn_4Sb_3, higher density provides higher value of Seebeck coefficient. Seebeck coefficients and electrical conductivities of near single-phase Zn_4Sb_3 (SC7HP2) were lower than possibly due to the presence of Zn. Seebeck coefficients and electrical conductivities in materials containing $\varepsilon+\beta$ phases (SC07HP2) were lowered possibly due to the presence of metallic ZnSb. In high-density, single-phase Zn_4Sb_3, thermoelectric power factor, $\theta(\mu W/cmK^2)$, which is a measure of thermoelectric efficiency parameter, was comparable with the material in reference [2]. Lower density resulted in lower thermoelectric power factor, as expected. The existence of Zn or ZnSb phase resulted in marked decrease in thermoelectric properties. Similar results showed that the addition of Zn up to 3 at.% exhibited semiconducting behavior, which changed to metallic for higher Zn contents [2].

Transport properties at room temperature in the single-phase (SC3HP2 and SC3HP24) and near single-phase (SC7HP2) materials are presented in Table 3. Positive values of Hall coefficient represent that the major carriers are holes in these materials indicating p-type conductivity. Hall mobility in the high-density, single-phase Zn_4Sb_3 (SC3HP24) sample is in good agreement with that of the reference material [2], and carrier concentrations are a little higher compared to that of the reference, indicating lower Seebeck coefficient. It is worth noting that higher carrier concentration for high-density, single-phase Zn_4Sb_3 (SC3HP24) does not provide higher electrical conductivity compared to that of the reference materials, presumably due to these samples still having a relatively lower density than that of reference material [2]. Low value of Hall mobility was measured in low-

Table 3 Transport properties at room temperature for Zn_4Sb_3 processed by the sintering of cold die-pressed compacts and hot pressing

Sample	Hall coefficient R_H (cm^3/C)	Hall mobility μ (cm^2/Vsec)	Carrier concentration p (cm^{-3})
Ref. [2]	–	30	9×10^{19}
SC3HP2	0.0223	11.12	2.80×10^{20}
SC3HP24	0.0635	29.47	9.83×10^{19}
SC7HP2	0.0318	8.93	1.97×10^{20}

density, single-phase Zn_4Sb_3 (SC3HP2), as well as in near single-phase Zn_4Sb_3 (SC7HP2). In single-phase Zn_4Sb_3, electrical conductivities did not vary much with density in single-phase materials, but Seebeck coefficient in low density sample (SC3HP2) was a little less than that of the high density sample (SC3HP24) due to high carrier concentration. Carrier concentrations in SC3HP2 and SC7HP2 samples are on the order of 10^{20}, which seems to be somewhat higher for the normal thermoelectric semiconductors, resulting in lower Seebeck coefficients. From discussions above, it is suggested that thermoelectric properties can be improved with higher density and single-phase Zn_4Sb_3.

Thermoelectric properties as a function of temperature for both single-phase SC3HP2 and SC3HP24 samples were investigated from room temperature to 600 K as shown in Figs. 8 and 9, respectively. Generally, Seebeck coefficients increased and electrical conductivities decreased with increasing temperature similarly to those for single-phase Zn_4Sb_3, where bipolar conduction seems to appear [2]. However, Seebeck coefficient in low-density, single-phase sample shows some fluctuation in the medium temperature range, resulting in a corresponding fluctuation in thermoelectric power factor as shown in Fig. 8a, c. Such a fluctuation is not generally shown in high-density, single-phase Zn_4Sb_3 [2, 3], but a similar result was found in a low-density MA Zn_4Sb_3, where the phase dissociated to ZnSb+Zn and the evaporation of the dissociated Zn occurred during one cycle of heating to 600 K, [13]. This is believed due to the relatively high surface area in the low density sample increasing the kinetics of phase dissociation. Fluctuation is greatly suppressed in the high-density sample, as shown in Fig. 9, suggesting that a higher density state provides better stability at high temperature.

Thermoelectric power factors up to 600 K were a little lower than those of the material in reference [2], possibly leading to a lower figure of merit (ZT). The thermal conductivity data were not measured in this study, so that direct estimation of ZT could not be made, however, assuming that thermal conductivities of our samples do not differ significantly from that of single-phase Zn_4Sb_3 [2], the ZTs in the specimens processed by the sintering of cold die-pressed compacts and hot pressing were estimated to be about 0.8 at 600 K, in Table 4. In the table, the properties of single-phase Zn_4Sb_3 produced by melting in an evacuated

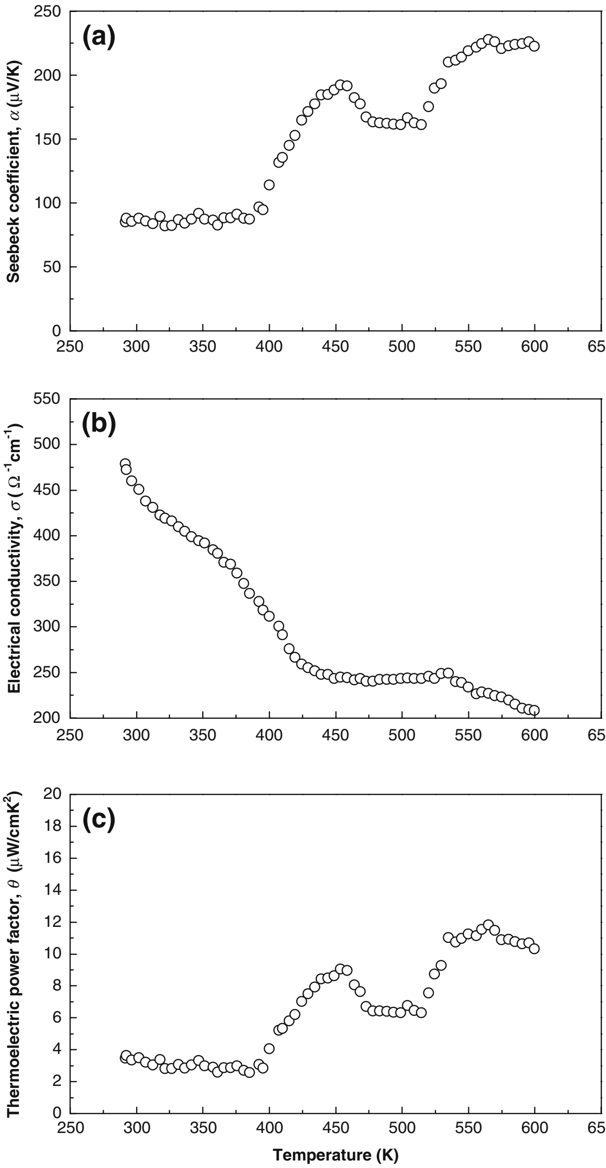

Fig. 8 Thermoelectric properties as a function of temperature in SC3HP2 specimen; (**a**) Seebeck coefficient, (**b**) electrical conductivity, (**c**) thermoelectric power factor

Table 4 Thermoelectric properties of specimens processed by sintering of cold die-pressed compact and hot pressing (at 600 K)

Sample	α (μV/K)	σ (Ω^{-1} cm^{-1})	θ (μW/cmK^2)	λ (mW/cmK)	ZT	Remarks
Ref. [2]	185	330	11.3	7	1	Measured
Ref. [3]	205	88	3.7	7^*	0.32	Estimated
SC3HP2	222.6	208.4	10.32	7^*	0.88	Estimated
SC3HP24	201.9	229.1	9.34	7^*	0.80	Estimated

*λ was Estimated from the graph of thermal conductivity as a function of temperature in ref. [2].

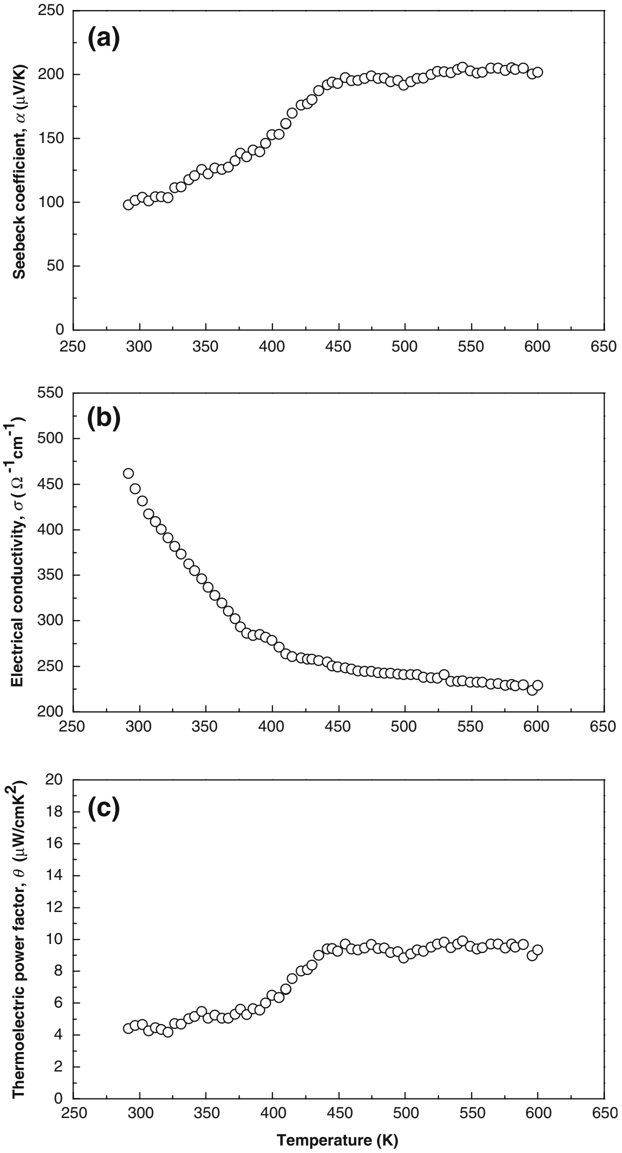

Fig. 9 Thermoelectric properties as a function of temperature in SC3HP24 specimen; (**a**) Seebeck coefficient, (**b**) electrical conductivity, (**c**) thermoelectric power factor

quartz ampoule followed by granulation and hot pressing [2], and those prepared by vacuum melting [3] are provided for references.

Summary

Single-phase Zn_4Sb_3 was successfully synthesized by the sintering of cold die-pressed compacts using a nominally 3.5 at.% Zn rich composition. Subsequent hot pressing produced single-phase, bulk Zn_4Sb_3 specimens without cracks. Electrical conductivity did not vary much with density in single-phase Zn_4Sb_3, but the Seebeck coefficient in the low-density sample was a little less than that for the high-density sample due to high carrier concentration. It is suggested that thermoelectric properties can be improved when higher density in single-phase Zn_4Sb_3 is provided in this processing. Hall mobilities are somewhat greater but carrier concentrations are less in single-phase Zn_4Sb_3 compared to the published data, indicating lower electrical conductivity and higher Seebeck coefficient. Thermoelectric power factors up to 600 K in Zn_4Sb_3 produced in this study are comparable to the published data for single-phase Zn_4Sb_3, and an estimated figure of merit is about 0.8 at 600 K. Synthesis by sintering of cold die-pressed compact and hot pressing offers a potential alternative processing route for this material system.

Acknowledgement This research was supported by the Regional Innovation Center (RIC) Program which was conducted by the Ministry of Commerce, Industry and Energy of the Korean Government.

References

1. Tapiero M, Tarabichi S, Gies JG, Noguet C, Zielinger JP, Joucla M, Loison JL, Robino M (1985) Solar Energy Mater 12:257
2. Caillat T, Fleurial J-P, Borshchevsky A (1997) J Phy Chem Solids 58(7):1119
3. Zhu TJ, Zhao XB, Yan M, Hu SH, Li T, Chou BC (2000) Mater Lett 46(1):44
4. Mayer HW, Mikhail I, Schubert K (1978) J Less Common Metals 59:43
5. Izard V, Record MC, Tedenac JC (2002) J Alloys Comp 345:257
6. Aizawa T, Iwaisako Y (1999) 18th International Conference on Thermoelectrics, Baltimore, Maryland, USA, August 29–September 2, pp 73–176
7. Souma T, Nakamoto G, Kurisu M (2002) J Alloys Comp 340(1/2):275
8. Prasad LC, Mikula A (2000) J Alloys Comp 299:175
9. Koch CC (1989) Annu Rev Mater Sci 121
10. Guo Q, Kleppa OJ (1995) J Alloys Comp 221(1/2):45
11. Battezzati L, Pappalepore P, Dubiano F, Gallino I (1999) Acta Mater 47(6):1901
12. Van der Pauw LJ (1958) Philips Res Reports 13(1):1
13. Ur S-C, Nash P, Kim I-H (2003) J of Mater Sci 38(17):3553